Current Filamentation in Large Bi_{2}Sr_{2}CaCu_{2}O_{8+δ} Mesa Devices Observed via Luminescent and Scanning Laser Thermal Microscopy

T. M. Benseman, A. E. Koshelev, V. Vlasko-Vlasov, Y. Hao, W.-K. Kwok, U. Welp, C. Keiser, B. Gross, M. Lange, D. Kölle, R. Kleiner, H. Minami, C. Watanabe, and K. Kadowaki

Phys. Rev. Applied **3**, 044017 — Published 27 April 2015

DOI: 10.1103/PhysRevApplied.3.044017

Current filamentation in large $Bi_2Sr_2CaCu_2O_{8+\delta}$ mesa devices observed via luminescent and scanning laser thermal microscopy

T. M. Benseman,[1,2] A. E. Koshelev,[1] V. Vlasko-Vlasov,[1] Y. Hao,[1,2] W.-K. Kwok,[1] U. Welp,[1] C. Keiser,[3] B. Gross,[4] M. Lange,[4] D. Kölle,[4] R. Kleiner,[4] H. Minami,[5] C. Watanabe,[5] and K. Kadowaki [5]

[1] Materials Science Division, Argonne National Laboratory, Argonne IL 60439

[2] Department of Physics, University of Illinois at Chicago, 845 W. Taylor St., Chicago IL 60607
[3] Northern Iowa University, Cedar Falls, IA 50614

[4] Physikalisches Institut and Center for Collective Quantum Phenomena in LISA$^+$, Universität Tübingen, Auf der Morgenstelle 14, D-72076 Tübingen, Germany

[5] Institute for Materials Science, University of Tsukuba, Ibaraki 305-8753, Japan

Abstract

We have studied the self-heating of a large stack of $Bi_2Sr_2CaCu_2O_{8+\delta}$ intrinsic Josephson junctions, of a configuration designed for THz generation. We find good qualitative agreement between direct thermoluminescent measurements of the device surface temperature and low-temperature scanning laser microscopy images. In particular, the two techniques both reveal a novel mode of thermal instability through the asymmetric nucleation of a small hot-spot near a corner/edge of the sample. This behavior conforms with a theoretical stability analysis, and the radius of the hot-spot is in excellent agreement with theoretical predictions, as is its growth with increasing bias current and bath temperature. Narrow hot-spots may offer a new possible means of enhancing the terahertz emission power from this type of device.

Introduction

Stacks of intrinsic Josephson junctions (IJJs) in the high-temperature superconductor $Bi_2Sr_2CaCu_2O_{8+\delta}$ [1] form a promising compact source of coherent terahertz radiation [2, 3]. For a number of reasons, it is essential to understand self-heating behavior in this type of device. Due to the low thermal conductivity of $Bi_2Sr_2CaCu_2O_{8+\delta}$ (Bi-2212) self-heating in large stacks of IJJs is substantial when they are biased to current-voltage conditions typical for THz generation [4-7]. Excessive self-heating may obviously be detrimental to THz emission, if the device entirely self-heats above its superconducting critical temperature. Theoretical predictions [6, 7] as well as experimental evidence [8, 9] suggest that a certain amount of self-heating may be beneficial for emission from these devices, especially if the resulting mesa temperature is very inhomogeneous. A localized thermal hot-spot may act as an internal resistive shunt, promoting phase-locking of the stacked junctions to the same voltage and THz emission frequency. Also, if the pattern of self-heating is highly asymmetric with respect to the cavity mode being excited, then coupling of the Josephson oscillations to free space – and thus the level of emitted THz power – is predicted to be strongly enhanced [10]. Localized hot-spots have been observed in low-temperature scanning laser thermal microscopy (LTSLM) studies [11-13] as well as in thermoluminescence imaging [14-16]. Indeed, the highest levels of THz power observed to date from Bi-2212 mesa devices [17, 18] occur in the presence of strong self-heating typical for hot-spot formation. However, recent thermal imaging experiments do not reveal a clear correlation between hot-spot formation and THz-emission [15, 16], whereas emission experiments under uniform and non-uniform biasing conditions indicate that an inhomogeneous temperature may benefit emission [19]. It is

therefore crucial to understand the complex dynamic states that arise from the coupling from highly non-uniform temperature distributions and the non-linear Josephson dynamics, as has been recently investigated numerically in a model of 1-D coupled sine-Gordon equations [20]. Here we present a thermal imaging study combining thermoluminescent micro-imaging and LTSLM on the same device. Both techniques yield the same results if the proper sensitivity function of LTSLM is taken into account. Furthermore, by careful heat-sinking of the sample we extend the range of thermal imaging to lower temperatures and observe a novel mode of thermal hot-spot dynamics. At low temperatures hot-spots with sizes that are significantly smaller than the sample size nucleate in a corner (at the edge) of the sample and undergo on increasing bias current a sequence of multistability and hysteretic jumps. Such findings are in agreement with model calculations of the stability of current filaments [21]. At higher temperatures the hot-spot size increases strongly resulting in a location near the center of the sample; and on further increasing temperature the hot-spot size would exceed the sample dimension and a thermal instability no longer occurs.

Experiment

The sample studied in this work is a Bi-2212 mesa of dimensions 300 × 60 × 0.8 μm^3 containing approximately 530 junctions, and patterned on the surface of an optimally-doped Bi-2212 crystal of ~4 μm thickness that has been soldered to a 0.5 mm thick Cu-substrate. In this mounting scheme epoxies are avoided enabling optimal heat removal from the mesa. At bath temperatures of around 60 K and under correct biasing conditions, it can generate up to 60 μW of coherent far-field radiation at approximately 0.6 THz [14].

In this work we investigate the unusual and complex current filamentation behavior, which this device exhibits at lower bath temperatures.

Bi-2212 is characterized by a rather poor *c*-axis thermal conductivity and a *c*-axis electrical conductivity, which strongly rises with increasing temperature. Therefore, under certain combinations of electrical biasing and heat transport, Bi-2212 mesas may undergo a thermal instability resulting in the formation of regions of strongly localized thermal runaway, associated with the appearance of so-called current filaments, which carry a much higher current density and which self-heat to a much higher temperature than the surrounding material. This phenomenon is not specific to superconductivity. It has been known in semiconducting materials since the 1930s [22] and the properties of current filaments have been extensively studied since then [21, 23-26]. If such filaments have a characteristic length scale which is significantly smaller than the dimensions of the device, then the device may exhibit the formation, migration, and switching behavior of hot-spots as shown in Figures 1 and 2 below. For the purposes of analytically understanding hot-spot behavior, a Bi-2212 mesa is equivalent to an electrically biased sheet of semiconducting material, as has been considered in detail by Volkov and Kogan [24]. Both materials are characterized by positive $d\sigma/dT$, an in-plane thermal conductivity κ_{ab}, and a heat removal coefficient P_0. For a Bi-2212 mesa device, heat removal occurs through the Bi-2212 base crystal [5] at a rate given by $P = P_0(T - T_0)$ where T is the (average) mesa temperature and T_0 the bath temperature.

A requirement for electrical multi-stability and current-filamentation to arise is the appearance of a branch in the current-voltage (*I-V*) characteristics with negative differential conductivity, such as in S- or N(Z)-shaped characteristics [25, 26]. Over-

heating in materials with $d\sigma/dT > 0$ typically results in S-shaped characteristics (see Fig. 1). Under voltage bias, this branch is not stable and bi-stability arises in which the current jumps to the upper (lower) branch at the turning points of the *I-V*. For sufficiently high load resistance *R* in the external circuit such that $R > R_c$, where R_c is the *c*-axis resistance of the mesa, the branch with negative differential conductivity is stable against uniform fluctuations and can in principle be traced out. However, this state may be unstable towards inhomogeneous fluctuations in which the current density and temperature become dependent on coordinates *x* and *y,* that is, towards the formation of hot-spots and current filaments. Stability analysis [21, 24] reveals that the minimum lateral dimension of the sample for an inhomogeneous state to occur is given as $l_c \approx \pi\sqrt{\kappa_{ab}\Big/\left(\sigma_c' E_c^2 - P_0/h_c\right)}$, where $E_c = V_{mesa}/h_c$ is the *c*-axis electric field, h_c the height of the mesa, σ_c is the *c*-axis conductivity and $\sigma_c' = \partial\sigma_c/\partial T$ its temperature derivative. Here, $\sigma_c' E_c^2 > P_0/h_c$, which is in fact the condition for a branch in the *I-V*-curve with negative differential conductivity to occur. The quantities in these expressions refer to the homogeneous state, which may be difficult to access experimentally since a sufficiently large sample is unstable against the formation of hot-spots. Alternatively, near the turning point of the *I-V*-characteristics one can obtain the temperature distribution through an expansion up to second order in temperature around a stable point on the lower branch of the *I-V*. In this way we obtain that a hot-spot in a strip-shaped sample has a characteristic half-width of $x_{hs} = \sqrt{\kappa_{ab}/\left(P_0/h_c - \sigma_c' E_c^2\right)}$, where the quantities are evaluated at the stable reference point. The mesa temperature around the hot-spot is approximately given by $T = T_1 + \left(T_2 - T_1\right)\Big/\cosh^2\left(x/2x_{hs}\right)$, where the hot-spot is centered at $x = 0$ with a central

temperature T_2, while T_1 is the mesa temperature far from the hot-spot. If the sample is larger than l_c in both in-plane directions, a two-dimensional hot-spot arises, and the heat diffusion equation must be solved numerically. A fit to the numerical solutions yields a hot-spot radius still approximately given by $r_{hs} \approx \sqrt{\kappa_{ab} / \left(P_0 / h_c - \sigma_c' E_c^2\right)}$ and an excess current drawn by the hot-spot of $I_{hs} = \iint\limits_{hot-spot} \{J_z[T(x,y)] - J_z[T_1]\}\, dxdy \approx 62\sigma_c' \kappa_{ab} / \sigma_c'' E_c$. In addition to materials parameters (κ_{ab} and σ_c'), the hot-spot size and the critical sample size depend sensitively on details of the experimental set-up through the heat removal coefficient P_0.

The two imaging techniques that we compare in this manuscript have been demonstrated previously, although not on the same device. Thermoluminescent micro-imaging (see Fig. 1a) has been employed for a number of applications in the past [27], while more recently we have used it for imaging self-heating in Bi-2212 mesas [14]. As described in [14] we take advantage of the temperature dependence of the 612 nm fluorescence line of the europium chelate compound europium thenoyltrifluoroacetonate (EuTFC). A recent variation of this technique employs a coating of SiC granules in place of the EuTFC film [15, 16]. The key advantage of thermoluminescent imaging is that it provides a direct quantitative map of the surface temperature of the sample.

As described in [11-13], LTSLM uses a modulated laser beam to induce a modulation of the voltage across a current-biased sample. LTSLM offers excellent sensitivity and spatial resolution, however, it is difficult to quantitatively convert these results into a sample temperature, since the observed signal depends not only upon the electrical conductivity derivative $\sigma_c'(x,y)$ and *c*-axis local current density $J_z(x, y)$, but also on the

thermal conductivities $\kappa_{ab}[T(x, y)]$ and $\kappa_c[T(x, y)]$ as well as weakly on the heat capacity $C_p[T(x, y)]$, which have their own temperature dependencies that could for example induce non-monotonic signals.

Figure 1 shows images collected on the same Bi-2212 mesa THz device via both techniques, for a range of currents, and at a bath temperature of 25 K. Figure 1 (d) and (e) show excellent qualitative agreement between the results of the two techniques. For bath temperatures of 45 K and above, thermal imaging reveals self-heating over a broad area of comparable size to the mesa itself, with self-heating strongest in the center of the mesa. This is similar to the results reported in [14] and the results of numerical simulations of Bi-2212 mesa self-heating [6, 7]. However, at bath temperatures of 35 K and below, a new type of behavior appears. For sufficiently large bias currents on the return leg of the *I-V* characteristic, (typically around 10 mA) a small hot-spot hysteretically nucleates as shown in Fig. 1 and Fig. 3a. At the lowest temperatures the hot-spot is clearly smaller than the sample width making it possible to explore its 2-D dynamics. The presence of the hot-spot results in a lower mesa resistance, which is the reason for the jumps seen in the *I-V* curves in Fig. 1a (inset) and Fig. 1b. As revealed by frames #1 and #2, the hot-spot nucleates upon a current increment of less than 0.2 mA, i.e., ~2 %, indicative of a true thermal instability. Also note that the temperature in the hot-spot jumps to close to T_c whereas over the majority of the mesa surface the temperature actually decreases (see traces 1 and 2 in Fig. 1c). This is consistent with the observation that roughly half the current is confined into the hot-spot (see Fig. 2b). The temperature variation in trace 1 of Fig. 1c is caused by lateral heat removal along the surface of the base crystal; for heat removal strictly along the *c*-axis a spatially uniform

temperature is expected. For certain currents and temperatures, the mesa may randomly jump between the hot-spot and no-hot-spot states, typically on a timescale of a few seconds (Fig. 2b, inset).

In the ANL thermoluminescence cryostat, the hot-spot was seen to nucleate at the corner of the mesa, while LTSLM images made in Tübingen show it nucleating along the edge of the mesa (cf. frame #2). This is likely to be due to subtle differences in the heat-sinking of the sample between the two cryostats. In fact, upon increasing temperature, the nucleation site of the hot-spot shifts along the edge and finally towards the center of the mesa (see Fig. 3a).

Between 40 and 65 mA there exist two hysteretic current-voltage paths, corresponding to the hot-spot located near the center of the mesa, or near the left end of the mesa as represented by frames #4 and #6 in Fig. 1d. (We note that this asymmetrical behavior is commonly seen in mesas with sufficiently strong heat removal. Further examples of the resulting thermal images are given in the Supplemental Material [28].) At currents above ~65 mA the thermal state of the mesa is reversible in current and characterized by very strong over-heating centered on the middle of the mesa. On decreasing current the hot-spot remains at the center of the mesa for currents larger than ~40 mA at which point it jumps to the end of the mesa. This jump is accompanied by a jump in the *I-V* curve, see inset (ii) in Fig. 1b. On subsequent increasing current, the hot-spot remains at the end of the mesa for currents up to ~60 mA.

A stability analysis of current filaments yielded the surprising result that a current filament is not stable in the interior of the sample (which is assumed to have convex boundaries) but is attracted to a corner or edge [21]. On a qualitative level, the nucleation

of a hot-spot at a corner can be explained by realizing that this hot-spot would require about ¼ of the current a similar hot-spot located in the center of the sample would draw. Thus, upon increasing the bias along an *I*-*V*-curve such as shown in Fig. 1b(i) the first (i.e., lowest bias current) instability that could arise is the nucleation of a corner hot-spot. With increasing current, hysteretic jumps between corner and edge filaments are expected to occur. Furthermore, the simulations show [21] that a current filament can be pinned near the center of the sample if an artificial seed of enhanced temperature is introduced, where the required temperature enhancement depends strongly on the sample size. Our thermal images at low temperature and low bias clearly reveal the nucleation of a corner filament, which with increasing bias current undergoes hysteretic jumps towards a center filament. Such a scenario can arise in a model in which the equilibrium position of the filament is determined by the competition between two energies, the attraction to the corner and the pinning at the location of enhanced background temperature near the center due to lateral cooling (see trace 1 in Fig. 1c). At low temperatures and low bias the attraction to the corner wins out whereas at high bias and elevated temperature pinning near the mesa center dominates. For mesas exhibiting stronger self-heating (e.g. those sitting on comparatively thick base crystals) the temperature pinning may always be sufficient to stabilize the hot-spot near the center of the mesa, even at the lowest power dissipation at which the hot-spot stably exists.

For optimally doped Bi-2212, $\sigma_c'(T)$ peaks at around 85 K. Consequently, LTSLM on Bi-2212 mesas typically gives its largest signal response near the edge of the hot-spot, since with increasing local device temperature $T(x, y)$, $\sigma_c'(x, y)$ may drop to near zero and even become negative. Thus the dark regions in the center of the mesa in Fig. 1e are in

fact hotter than the surrounding lighter-shaded regions, as confirmed by our thermoluminescence results, and the wave-like features (for instance at bias currents of 29.95 and 22.33 mA) are in fact a consequence of the temperature dependent sensitivity of LTSLM.

At comparatively small bias voltages, the mesa current is an accelerating function of bias voltage (i.e. $d^2I/dV^2 \geq 0$ at bias currents below the backbending point seen in the inset of Fig. 1a). We may thus estimate the mesa conductance with negligible self-heating as being the tangent to the *I-V* characteristic in this region (black lines on plot) as described in [14], allowing us to determine $\sigma_c(T)$ below T_c, and convert our temperature maps into maps of the *c*-axis quasiparticle current density.

The hot-spot was imaged at the minimum current at which it was stable, at bath temperatures between 6 K and 35 K, as well as at 45 K (see Fig. 3a), at which temperature the hot-spot becomes comparable to the width of the mesa itself, and there still exists a cusp – but no hysteretic jump – in the *I-V* characteristic. We suggest that at a temperature near 45 K the character of the hot-spot in the present device changes from two-dimensional to one-dimensional. At higher temperatures there are no features in the *I-V* curves discernable (see Fig. 1a) and the thermal images reveal a broad temperature distribution consistent with simulations [6]. Figure 2a shows temperature cross-sections of the hot-spot in these states, while Fig. 2b compares predicted r_{hs} and I_{hs} (as respectively calculated from the relations given above with values measured experimentally. r_{hs} was measured from Fig. 2a, while I_{hs} was obtained from the maps of $J_z(x, y, T_{bath})$ plotted in Fig. 3. In this calculation, $\kappa_{ab}(\overline{T}_{hs})$ and $\sigma_c'(\overline{T}_{hs})$ were taken averaging $T(x, y)$ over $r < r_{hs}$, while $\kappa_{ab}(T)$ for optimally doped Bi-2212 was taken from

[29]. From the resistance vs. temperature curve and *I-V* characteristics plotted in Fig. 1a, the average power density and average temperature rise in the mesa can be obtained, allowing the heat removal coefficient P_0 to be estimated for small bias currents at which $T(x, y)$ is still comparatively uniform. P_0 varies with temperature, but is typically around 6×10^4 $Wm^{-2} K^{-1}$, consistent with the mesa being heat sunk to the metal substrate through a base crystal around 4 microns thick, assuming that $\kappa_{ab}/\kappa_c \approx 10$ [6]. For temperatures at which the hotspot was close to the corner of the mesa, I_{hs} was calculated from the quadrant located entirely inside the mesa, and normalized accordingly to allow comparison with theory. Given the approximations necessarily made in these calculations, the close and systematic agreement between the theoretical and experimental values for hot-spot size and current, and their growth with increasing T_{bath} – as indicated in Fig. 2b – is remarkable. In the center of the hot-spot, local thermal runaway results in a current density up to seven times higher than J_z far from the hotspot. Despite this, the comparatively small area of the hot-spot means that it draws only 20 – 50% of the entire current driven through the mesa. The data in Fig. 2b suggest that the maximum temperature at which a hot-spot can still be observed is reached when the minimum hot-spot radius becomes larger than the width of the mesa. At higher temperatures the sample cannot accommodate the hot-spot anymore and the thermal instability does not occur.

Discussion and Conclusions

The behavior shown by this type of current filament may have significant implications for the design of IJJ THz sources in future. A hot-spot which is intrinsically narrow may

act as an effective shunt resistance for the stack of IJJs as described previously, without substantially disrupting the resonant properties of the remainder of the cavity. In fact, a certain degree of dissipation induced by the shunt may be beneficial for synchronizing the junctions and achieving high emission power from stacks of intrinsic junctions [6] as well as from arrays of conventional junctions [30]. Furthermore, a hot-spot which stably locates itself at one edge of the mesa will inherently make the Josephson critical current density asymmetric, which is predicted to strongly enhance the emission power [10]. If a mesa were to be designed such that its cavity resonance occurs at the same bath temperature and *I-V* conditions at which a sufficiently small hot-spot nucleates, then the hot-spot behavior observed here could be exploited for the purposes of enhanced THz emission.

We have measured the self-heating of a large Bi-2212 mesa device via two different techniques. We find good qualitative agreement between our direct thermoluminescent measurements of device surface temperature and our LTSLM images, confirming that the latter are primarily probing temperature-dependent changes in $\partial\sigma_c/\partial T$. In particular, the two techniques both reveal the asymmetric nucleation of a small asymmetric hot-spot at low mesa temperatures where the hot-spot diameter is significantly smaller than the mesa width. The nucleation / annihilation of the hot-spot causes dramatic hysteretic jumps in the mesa resistance. We find that the radius of this hot-spot is in excellent agreement with theoretical predictions, as is its growth with increasing bias current and bath temperature.

Acknowledgements

This research was supported by the Department of Energy, Office of Basic Energy Sciences, under Contract No. DE-AC02-06CH11357, by the Deutsche Forschungsgemeinschaft (Project KL 930/13-1), and by the Japanese Society for the Promotion of Science.

References

[1] R. Kleiner, F. Steinmeyer, G. Kunkel, and P. Müller, Intrinsic Josephson Effects in $Bi_2Sr_2CaCu_2O_8$ Single Crystals, Phys. Rev. Lett. **68**, 2394 (1992).

[2] L. Ozyuzer, A. E. Koshelev, C. Kurter, N. Gopalsami, Q. Li, M. Tachiki, K. Kadowaki, T. Yamamoto, H. Minami, H. Yamaguchi, T. Tachiki, K. E. Gray, and W.-K. Kwok, U. Welp, Emission of Coherent THz Radiation from Superconductors, Science **318**, 1291 (2007).

[3] U. Welp, K. Kadowaki, R. Kleiner, Superconducting emitters of THz radiation, Nat. Photonics **7**, 702 (2013).

[4] C. Kurter, K. E. Gray, J. F. Zasadzinski, L. Ozyuzer, A. E. Koshelev, Q. Li, T. Yamamoto, K. Kadowaki, W.-K. Kwok, M. Tachiki, U. Welp, Thermal Management in Large Bi2212 Mesas Used for Terahertz Sources, IEEE Appl. Superconductivity **19**, 428 (2009); C. Kurter, L. Ozyuzer, T. Proslier, J. F. Zasadzinski, D. G. Hinks, K. E. Gray, Counterintuitive consequence of heating in strongly-driven intrinsic junctions of $Bi_2Sr_2CaCu_2O_{8+\delta}$ mesas, Phys. Rev. B **81**, 224518 (2010); M. Suzuki, T. Watanabe, A. Matsuda, Interlayer Tunneling Spectroscopy for Slightly Overdoped $Bi_2Sr_2CaCu_2O_{8+\delta}$, Phys. Rev. Lett. **82**, 5361 (1999); H. B. Wang, T. Hatano, T. Yamashita, P. H. Wu, P. Müller, Direct observation of self-heating in intrinsic Josephson junction array with a nanoelectrode in the middle, Appl. Phys. Lett. **86**, 023504 (2005); V. N. Zavaritsky, Intrinsic Tunneling or Joule Heating?, Phys. Rev. Lett. **92**, 259701 (2004); V. M. Krasnov, M. Sandberg, I. Zogaj, *In situ* Measurement of Self-Heating in Intrinsic

Tunneling Spectroscopy, Phys. Rev. Lett., **94**, 077003, (2005), A. Yurgens, Supercond. Sci. Technol. **13**, R85 (2000).

[5] J. C. Fenton, C. E. Gough, Heating in mesa structures, J. Appl. Phys. **94**, 4665 (2003).

[6] A. Yurgens, Temperature distribution in a large $Bi_2Sr_2CaCu_2O_{8+\delta}$ mesa, Phys. Rev. B **83**, 184501 (2011).

[7] B. Gross, S. Guenon, J. Yuan, M. Y. Li, J. Li, A. Ishii, R. G. Mints, T. Hatano, P. H. Wu, D. Kölle, H. B. Wang, R. Kleiner, Hot-spot formation in stacks of intrinsic Josephson junctions in $Bi_2Sr_2CaCu_2O_8$, Phys. Rev. B **86**, 094524 (2012).

[8] M. Li, J. Yuan, N. Kinev, J. Li, B. Gross, S. Guenon, A. Ishii, K. Hirata, T. Hatano, D. Kölle, R. Kleiner, V. P. Koshelets, H. B. Wang and P. Wu, Linewidth dependence of coherent terahertz emission from $Bi_2Sr_2CaCu_2O_8$ intrinsic Josephson junction stacks in the hot-spot regime, Phys. Rev. B **86**, 060505(R) (2012).

[9] I. Kakeya, Y. Omukai, T. Yamamoto, K. Kadowaki, M. Suzuki, Effect of thermal inhomogeneity for terahertz radiation from intrinsic Josephson junction stacks of $Bi_2Sr_2CaCu_2O_{8+\delta}$, Appl. Phys. Lett. **100**, 242603 (2012).

[10] A. E. Koshelev, L. N. Bulaevskii, Resonant electromagnetic emission from intrinsic Josephson-junction stacks with laterally modulated Josephson critical current, Phys. Rev. B **77**, 014530 (2008); A. E. Koshelev, Alternating dynamic state self-generated by internal resonance in stacks of intrinsic Josephson junctions, Phys. Rev. B **78**, 174509 (2008).

[11] H. B. Wang, S. Guenon, J. Yuan, A. Iishi, S. Arisawa, T. Hatano, T. Yamashita, D. Kölle, and R. Kleiner, Hot Spots and Waves in $Bi_2Sr_2CaCu_2O_8$ Intrinsic Josephson

Junction Stacks: A Study by Low Temperature Scanning Laser Microscopy, Phys. Rev. Lett. **102**, 017006 (2009).

[12] H. B. Wang, S. Guenon, B. Gross, J. Yuan, Z. G. Jiang, Y. Y. Zhong, M. Grünzweig, A. Iishi, P. H. Wu, T. Hatano, D. Kölle, and R. Kleiner, Coherent Terahertz Emission of Intrinsic Josephson Junction Stacks in the Hot Spot Regime, Phys. Rev. Lett. **105**, 057002 (2010).

[13] S. Guénon, M. Gru□nzweig, B. Gross, J. Yuan, Z. G. Jiang, Y. Y. Zhong, M. Y. Li, A. Iishi, P. H. Wu, T. Hatano, R. G. Mints, E. Goldobin, D. Kölle, H. B. Wang, R. Kleiner, Interaction of hot spots and terahertz waves in $Bi_2Sr_2CaCu_2O_8$ intrinsic Josephson junction stacks of various geometry, Phys. Rev. B **82**, 214506 (2010).

[14] T. M. Benseman, A. E. Koshelev, W.-K. Kwok, U. Welp, V. K. Vlasko-Vlasov, K. Kadowaki, H. Minami, and C. Watanabe, Direct imaging of hot spots in $Bi_2Sr_2CaCu_2O_{8+\delta}$ mesa terahertz sources, J. Appl. Phys. **113**, 133902 (2013).

[15] H. Minami, C. Watanabe, K. Sato, S. Sekimoto, T. Yamamoto, T. Kashiwagi, R. A. Klemm, and K. Kadowaki, Local SiC photoluminescence evidence of hot spot formation and sub-THz coherent emission from a rectangular $Bi_2Sr_2CaCu_2O_{8+\delta}$ mesa, Phys. Rev. B **89**, 054503 (2014).

[16] C. Watanabe, H. Minami, T. Yamamoto, T. Kashiwagi, R. A. Klemm, K. Kadowaki, Spectral investigation of hot spot and cavity resonance effects on the terahertz radiation from high-T_c superconducting $Bi_2Sr_2CaCu_2O_{8+\delta}$ mesas, J. Phys.: Condens. Matter **26**, 172201 (2014).

[17] T. M. Benseman, K. E. Gray, A. E. Koshelev, W.-K. Kwok, U. Welp, H. Minami, K. Kadowaki, and T. Yamamoto, Powerful terahertz emission from $Bi_2Sr_2CaCu_2O_{8+\delta}$ mesa arrays, Appl. Phys. Lett. **103**, 022602 (2013).

[18] D. Y. An, J. Yuan, N. Kinev, M. Y. Li, Y. Huang, M. Ji, H. Zhang, Z. L. Sun, L. Kang, B. B. Jin, J. Chen, J. Li, B. Gross, A. Ishii, K. Hirata, T. Hatano, V. P. Koshelets, D. Kölle, R. Kleiner, H. B. Wang, W. W. Xu and P. H. Wu, Terahertz emission and detection both based on high-T_c superconductors: Towards an integrated receiver, Appl. Phys. Lett. **102**, 092601 (2013).

[19] M. Tsujimoto, H. Kambara, Y. Maeda, Y. Yoshioka, Y. Nakagawa, I. Kakeya, Dynamic Control of Temperature Distributions in Stacks of Intrinsic Josephson Junctions in $Bi_2Sr_2CaCu_2O_{8+\delta}$ for Intense Terahertz Radiation, Phys. Rev. Applied **2**, 044016 (2014).

[20] F. Rudau, M. Tsujimoto, B. Gross, T. E. Judd, R. Wieland, E. Goldobin, N. Kinev, J. Yuan, Y. Huang, M. Ji, X. J. Zhou, D. Y. An, A. Ishii, R. G. Mints, P. H. Wu, T. Hatano, H. B. Wang, V. P. Koshelets, D. Kölle, and R. Kleiner, Thermal and electromagnetic properties of $Bi_2Sr_2CaCu_2O_8$ intrinsic Josephson junction stacks studied via one-dimensional coupled sine-Gordon equations, arXiv:1412.0479v1.

[21] A. Alekseev, S. Bose, P. Rodin, E. Schöll, Stability of current filaments in a bistable semiconductor system with global coupling, Phys. Rev. E **57**, 2640 (1998).

[22] H. Lüder, E. Spenke, Über den Einfluß der Wärmeableitung auf das elektrische Verhalten von temperaturabhängigen Widerständen, Physikalische Zeitschrift **36**, 767 (1936).

[23] B. K. Ridley, Specific Negative Resistance in Solids, Proc. Phys. Soc. **82**, 954 (1963); K. D. Tsendin and A. B. Shmelkin, Conditions Preventing Thermal Breakdown in Semiconductor Devices, Technical Physics Letters, **30**, 525 (2004); M. Büttiker, H. Thomas, Bifurcation and Stability of Dynamical Structures at a Current Instability, Z. Phys. B **34**, 301 (1979); F. J. Niedernostheide, B. S. Kerner, H.-G. Purwins, Spontaneous appearance of rocking localized current filaments in a nonequilibrium distributive system, Phys. Rev. B **46**, 7559 (1992); P. Rodin, Theory of traveling filaments in bistable semiconductor structures, Phys. Rev. B **69**, 045307 (2004).

[24] A. F. Volkov and S. M. Kogan, Nonuniform Current Distribution in Semiconductors with Negative Differential Conductivity, J. Exp. Theor. Phys. (U.S.S.R.) **52**, 1647 (1967).

[25] A. F. Volkov, S. M. Kogan, Physical Phenomena in Semiconductors with Negative Differential Conductivity, Soviet Phys. Uspekhi **11**, 881 (1969); A. Wacker, E. Schöll, Criteria for stability in bistable electrical devices with S- or Z-shaped current voltage characteristic, J. Appl. Phys. **78**, 7352 (1995).

[26] A. V. Gurevich, R. G. Mints, Self-heating in normal metals and superconductors, Rev. Mod. Phys. **59**, 941 (1987).

[27] P. Kolodner and J. A. Tyson, Microscopic fluorescent imaging of surface temperature profiles with 0.01 °C resolution, Appl. Phys. Lett. **40**, 782 (1982); P. Kolodner and J. A. Tyson, Remote thermal imaging with 0.7-μm spatial resolution using temperature-dependent fluorescent thin films, Appl. Phys. Lett. **42**, 117 (1983); G. Hampel, P. Kolodner, P. L. Gammel, P. A. Polakos, E. de Obaldia, P. M. Mankiewich, A. Anderson, R. Slattery, D. Zhang, G. C. Liang, and C.F. Shih, High power failure of superconducting microwave filters: Investigation by means of thermal imaging, Appl.

Phys. Lett. **69**, 571 (1996); O. Haugen, T. H. Johansen, H. Chen, V. Yurchenko, P. Vase, D. Winkler, B. A. Davidson, G. Testa, E. Sarnelli, and E. Altshuler, High Resolution Thermal Imaging of Hotspots in Superconducting Films, IEEE Trans. Appl. Supercond. **17**, 3215 (2007); S. Niratisairak, O. Haugen, T. H. Johansen, and T. Ishibashi, Observation of hotspot in BSCCO thin film structure by fluorescent thermal imaging, Physica C **468**, 442 (2008).

[28] See Supplemental Material at [URL to be inserted by publisher] for additional examples of thermal images showing hotspot nucleation in another $Bi_2Sr_2CaCu_2O_8$ mesa device.

[29] K. Krishana, N. P. Ong, Q. Li, G. D. Gu, N. Koshizuka, Plateaus Observed in the Field Profile of Thermal Conductivity in the Superconductor $Bi_2Sr_2CaCu_2O_8$, Science **277**, 83 (1997).

[30] P. Hadley, M. R. Beasley, K. Wiesenfeld, Phase locking of Josephson-junction series arrays, Phys. Rev. B **38**, 8712-8719 (1988).

Figure captions

Figure 1

(a) Main image: $R(T)$ for Bi-2212 mesa (red solid curve) measured in absence of self-heating, using 10 μA bias current. Values for $T < T_c$ (blue squares) were determined by extrapolating from the slope of the low-bias *I-V* characteristic (black lines in inset). Dotted line is a fit of the form $R_c(T) = T^{-\alpha} P(T)$ used to interpolate between these two types of data. $P(T)$ is a 7th-order polynomial. Inset: *I-V* curves on downward current sweep at 5 K bath temperature intervals between 10 K and 100 K. (b) *I-V* curve for device at a bath temperature of 25 K. Black arrows indicate current sweep direction. These *I-V* curves present the lower half of typical S-shaped *I-V* curves, the upper portion cannot be reached due to limits on the current the device can carry. Insets (i) and (ii) show regions of *I-V* characteristic where it is hysteretic due to nucleation and relocation of hotspot, respectively. (c) Longitudinal temperature profiles of mesa, taken through centerline of hotspot in selected images from (e), which are temperature maps of mesa surface obtained by thermoluminescent imaging. Note the distinct hotspot (2) and no-hotspot states (1) which exist for certain currents. Reflection of excitation light off vertical surfaces results in artifacts in the images at the edges of the mesa and the electrode. (d) Left-most image is a conventional optical micrograph of mesa, showing the Au thin-film electrode (500 nm thick) extending from top end of the device. Black-and-white images are LTSLM raster scans of the mesa at the same set of bias currents. No LTSLM signal is seen for the top area of the mesa. Here the Au electrode almost

completely reflects the incident laser beam and prevents it from thermally coupling to the device.

Figure 2

(a) Longitudinal thermal cross-section of mesa, taken through centerline of hotspot at its minimum stable size at each bath temperature. (At 45 K there is no longer a distinct hotspot state, and no corresponding *I*-*V* jumps.)

(b) Main image: Hotspot radius r_{hs} (squares, solid lines) and excess current I_{hs} (circles, dashed lines) plotted against T_{bath}. Experimental values are plotted as squares and circles, while triangles are predictions calculated using the relations given in the main text. Inset: Random switching of mesa voltage, at T_{bath} = 40 K, corresponding to continual switching of mesa in and out of hotspot state.

Figure 3:

(a) Current density maps calculated from thermoluminescent images of smallest stable hotspot. (b) Corresponding maps in no-hotspot state at same I_{mesa}, T_{bath}.

Figures

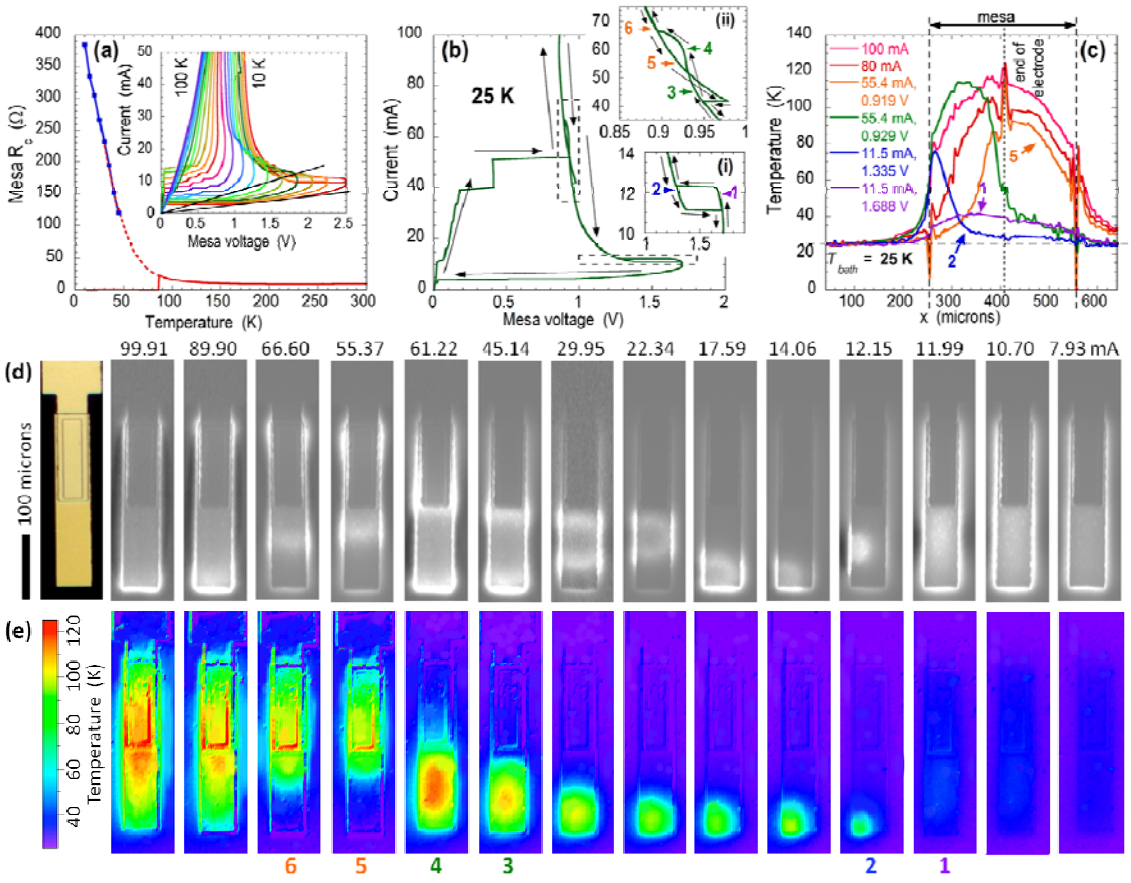

Figure 1 [color online only, intended as two-column figure]

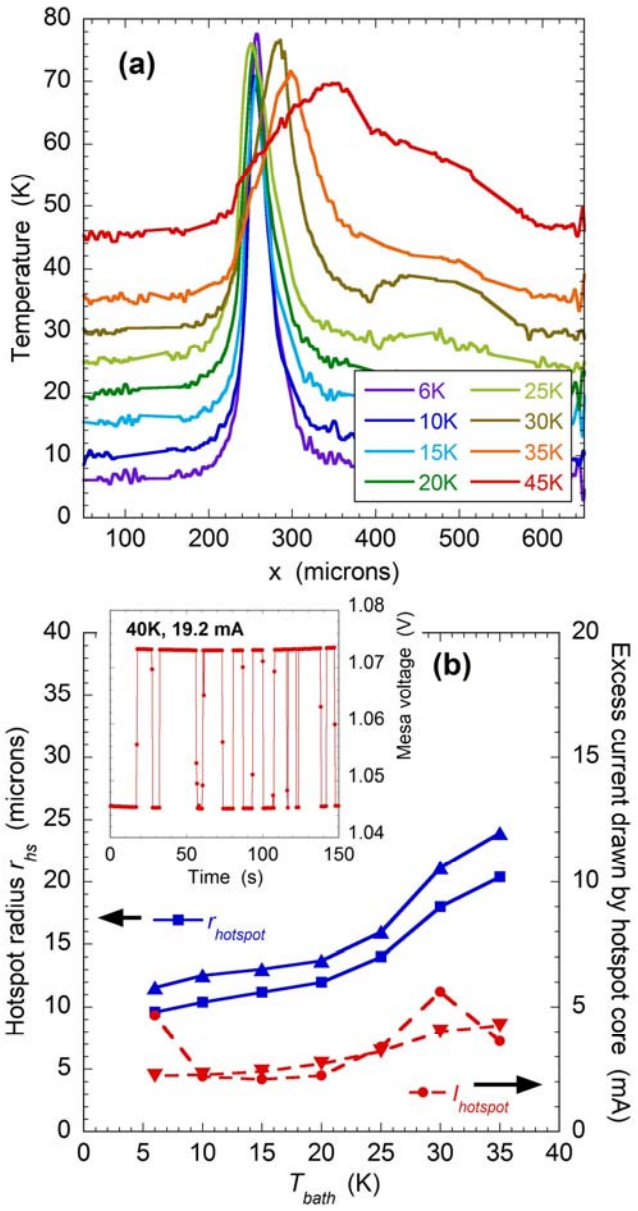

Figure 2 [color online only]

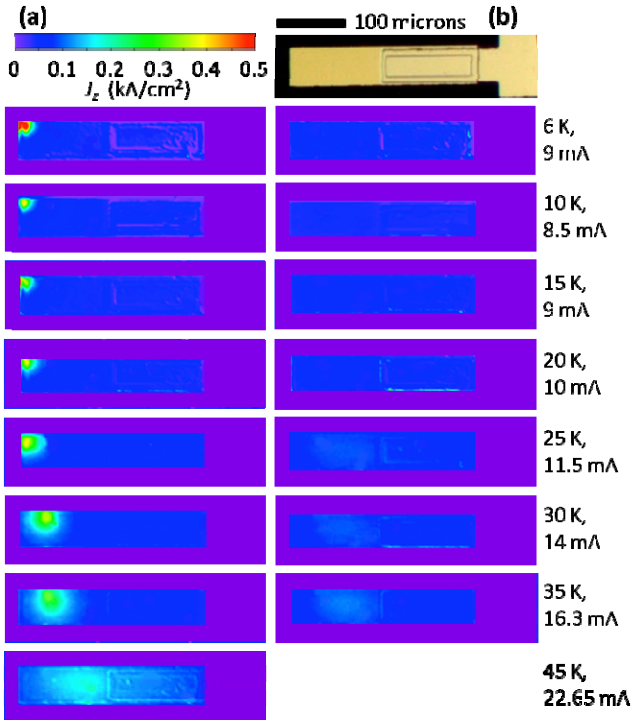

Figure 3 [color online only]